J|A|C|S ARTICLES

Published on Web 11/08/2008

Platinum(II) Complexes with Dipyridophenazine Ligands as Human Telomerase Inhibitors and Luminescent Probes for G-Quadruplex DNA

Dik-Lung Ma, Chi-Ming Che,* and Siu-Cheong Yan

Department of Chemistry and Open Laboratory of Chemical Biology of the Institute of Molecular Technology for Drug Discovery and Synthesis, The University of Hong Kong, Pokfulam Road, Hong Kong

Received August 1, 2008; E-mail: cmche@hku.hk

Abstract: A series of platinum(II) complexes containing dipyridophenazine (dppz) and C-deprotonated 2-phenylpyridine (N^CH) ligands were prepared and assayed for G-quadruplex DNA binding activities. $[Pt^{II}(dppz\text{-}COOH)(N^{\wedge}C)]CF_3SO_3$ (**1**; dppz-COOH = 11-carboxydipyrido[3,2-*a*:2′,3′-*c*]phenazine) binds G-quadruplex DNA through an external end-stacking mode with a binding affinity of $\sim 10^7$ dm^3 mol^{-1}. G-quadruplex DNA binding is accompanied by up to a 293-fold increase in the intensity of photoluminescence at $\lambda_{max} = 512$ nm. Using a biotinylated-primer extension telomerase assay, **1** was shown to be an effective inhibitor of human telomerase in vitro, with a $^{tel}IC_{50}$ value of 760 nM.

Introduction

There has been considerable interest in the study of G-quadruplex DNA (Figure 1) due to its involvement in the regulation of telomerase activities.[1−5] Human telomeric DNA is composed of a repeated double-stranded $[TTAGGG/CCCTAA]_n$ sequence except in the 3′-terminal region, which consists of a single-stranded tandem [TTAGGG] repeated sequence over several hundred bases.[6−9] In normal cells, approximately 100 bases will be lost during every cell division, leading to a gradual shortening of the telomere. In cancer cells, the telomeric length is maintained by telomerase, and the telomerase activity is expressed in over 90% of tumor cell lines but in relatively few normal cell types.[9] Thus, the inhibition of telomerase activity by inducing/stabilizing G-quadruplex formation and the detection of G-quadruplex DNA are important targets for developing new anticancer drugs.[1−5,10,11] Planar π-conjugated molecules such as cationic porphyrins are known to bind to and stabilize G-quadruplex DNA, resulting in antitelomerase activity, which triggers telomere shortening and cell growth suppression and subsequently leads to cell death.[12]

To date, a number of platinum(II) complexes have been reported as potent telomerase inhibitors. Lippard and co-workers have shown that cisplatin and its derivatives have antitelomerase activity.[13,14] The modes of action of these platinum(II) complexes are distinct from those of other G-quadruplex-interacting compounds, such as acridine derivatives, ethidium derivatives, quinolines, 9-anilinoproflavine, triazines, fluoroquinophenoxazines, telomestatin, and pentacyclic acridines.[12] Platinum(II)

(1) Mergny, J.-L.; Hélène, C. *Nat. Med.* **1998**, *4*, 1366.
(2) Jenkins, T. C. *Curr. Med. Chem.* **2000**, *7*, 99.
(3) Kerwin, S. M. *Curr. Pharm. Des.* **2000**, *6*, 441.
(4) Han, H.; Hurley, L. H. *Trends Pharmacol. Sci.* **2000**, *21*, 136.
(5) (a) Kelland, L. R. *Anticancer Drugs* **2000**, *11*, 503. (b) Rowley, P. T.; Tabler, M. *Anticancer Res.* **2000**, *20*, 4419. (c) Neidle, S.; Parkinson, G. *Nat. Rev. Drug Discovery* **2002**, *1*, 383. (d) Mokbel, K. *Curr. Med. Res. Opin.* **2003**, *19*, 470. (e) Riou, J.-F. *Curr. Med. Chem. Anti-Cancer Agents* **2004**, *4*, 439. (f) Kelland, L. R. *Eur. J. Cancer* **2005**, *41*, 971. (g) Sharma, S.; Doherty, K. M.; Brosh, R. M., Jr. *Curr. Med. Chem. Anti-Cancer Agents* **2005**, *5*, 183. (h) Petraccone, L.; Barone, G.; Giancola, C. *Curr. Med. Chem. Anti-Cancer Agents* **2005**, *5*, 463.
(6) McElligott, R.; Wellinger, R. J. *EMBO J.* **1997**, *16*, 3705.
(7) Wright, W. E.; Tesmer, V. M.; Huffman, K. E.; Levene, S. D.; Shay, J. W. *Gene Dev.* **1997**, *11*, 2801.
(8) Huffman, K. E.; Levene, S. D.; Tesmer, V. M.; Shay, J. W.; Wright, W. E. *J. Biol. Chem.* **2000**, *275*, 19719.
(9) Kim, N. W.; Piatyszek, M. A.; Prowse, K. R.; Harley, C. B.; West, M. D.; Ho, P. L.; Coviello, G. M.; Wright, W. E.; Weinrich, S. L.; Shay, J. W. *Science* **1994**, *266*, 2011.
(10) Cairns, D.; Anderson, R. J.; Perry, P. J.; Jenkins, T. C. *Curr. Pharm. Des.* **2002**, *8*, 2491.
(11) (a) Shin-ya, K.; Wierzba, K.; Matsuo, K.-I.; Ohtani, T.; Yamada, Y.; Furihata, K.; Hayakawa, Y.; Seto, H. *J. Am. Chem. Soc.* **2001**, *123*, 1262. (b) Missailidis, S.; Stanslas, J.; Modi, C.; Ellis, M. J.; Robins, R. A.; Laughton, C. A.; Stevens, M. F. *Oncol. Res.* **2002**, *13*, 175. (c) Burger, A. M.; Dai, F.; Schultes, C. M.; Reszka, A. P.; Moore, M. J.; Double, J. A.; Neidle, S. *Cancer Res.* **2005**, *65*, 1489. (d) Pennarun, G.; Granotier, C.; Gauthier, L. R.; Gomez, D.; Hoffschir, F.; Mandine, E.; Riou, J.-F.; Mergny, J.-L.; Mailliet, P.; Boussin, F. D. *Oncogene* **2005**, *24*, 2917. (e) Tahara, H.; Shin-ya, K.; Seimiya, H.; Yamada, H.; Tsuruo, T.; Ide, T. *Oncogene* **2006**, *25*, 1955. (f) Gomez, D.; O'Donohue, M. F.; Wenner, T.; Douarre, C.; Macadé, J.; Koebel, P.; Giraud-Panis, M. J.; Kaplan, H.; Kolkes, A.; Shin-ya, K.; Riou, J.-F. *Cancer Res.* **2006**, *66*, 6908. (g) Jantos, K.; Rodriguez, R.; Ladame, S.; Shirude, P. S.; Balasubramanian, S. *J. Am. Chem. Soc.* **2006**, *128*, 13662. (h) Franceschin, M.; Rossetti, L.; D'Ambrosio, A.; Schirripa, S.; Bianco, A.; Ortaggi, G.; Savino, M.; Schultes, C.; Neidle, S. *Bioorg. Med. Chem. Lett.* **2006**, *16*, 1707. (i) Ou, T.-M.; Lu, Y.-J.; Zhang, C.; Huang, Z.-S.; Wang, X.-D.; Tan, J.-H.; Chen, Y.; Ma, D.-L.; Wong, K.-Y.; Tang, J. C.-O.; Chan, A. S.-C.; Gu, L.-Q. *J. Med. Chem.* **2007**, *50*, 1465. (j) De Cian, A.; DeLemos, E.; Mergny, J.-L.; Teulade-Fichou, M.-P.; Monchaud, D. *J. Am. Chem. Soc.* **2007**, *129*, 1856. (k) Brassart, B.; Gomez, D.; De Cian, A.; Paterski, R.; Montagnac, A.; Qui, K. H.; Temime-Smaali, N.; Trentesaux, C.; Mergny, J. L.; Gueritte, F.; Riou, J. F. *Mol. Pharmacol.* **2007**, *72*, 631. (l) Fu, B.; Huang, J.; Ren, L.; Weng, X.; Zhou, Y.; Du, Y.; Wu, X.; Zhou, X.; Yang, G. *Chem. Commun.* **2007**, *31*, 3264. (m) Ma, D.-L.; Lai, T.-S.; Chan, F.-Y.; Chung, W.-H.; Abagyan, R.; Leung, Y.-C.; Wong, K.-Y. *ChemMedChem* **2008**, *3*, 881. (n) Lu, Y.-J.; Ou, T.-M.; Tan, J.-H.; Peng, D.; Sun, N.; Wang, X.-D.; Shao, W.-Y.; Wu, W.-B.; Huang, Z.-S.; Bu, X.-Z.; Ma, D.-L.; Wong, K.-Y.; Gu, L.-Q. *J. Med. Chem.* **2008**, *51*, 6381.

Table 1. UV−Vis Absorption Data of **1**−**5** in CH_3CN at 20 °C

complex	UV−vis λ/nm (ε_{max}/dm^3 mol^{-1} cm^{-1})
1	407 (sh, 2.88 × 10^3), 382 (br, 3.55 × 10^3), 321 (1.43 × 10^4), 251 (3.85 × 10^4)
2	402 (sh, 1.60 × 10^3), 387 (4.61 × 10^3), 367 (4.04 × 10^3), 288 (1.63 × 10^4)
3	410 (sh, 2.03 × 10^3), 390 (8.23 × 10^3), 370 (6.74 × 10^3), 275 (2.47 × 10^4)
4	447 (sh, 1.05 × 10^3), 380 (5.87 × 10^3), 361 (6.16 × 10^3), 281 (2.30 × 10^4)
5	416 (sh, 1.65 × 10^3), 369 (br, 5.14 × 10^3), 269 (1.79 × 10^4)

complexes containing aromatic diimine ligands are also known to bind to DNA.[15−17]The earliest examples, $[Pt(terpy)X]^+$ (terpy = 2,2′:6′,2″-terpyridine; X = Cl, SR) and their derivatives $[Pt(terpy)L]^{n+}$ [18] (L = anionic ligand, n = 1; L = neutral ligand, n = 2), were shown to bind to DNA mainly by intercalation. As pioneered by Barton and co-workers, octahedral metal complexes (such as ruthenium(II) and rhodium(III) complexes) containing dppz ligand (dppz = dipyrido[3,2-*a*:2′,3′-*c*]phenazine) are good metallointercalators of double-stranded DNA.[19]

We conceive that platinum(II) complexes of dppz ligands would be of interest for DNA binding studies, as they would possess a planar Pt^{II} coordination geometry as well as flat aromatic dppz ligands.[15d,17c] Furthermore, platinum(II) complexes containing aromatic diimine ligands have rich photoluminescent properties, which are strongly affected by subtle changes of their local environment and can therefore be used for luminescent signaling studies.[20] While there have been extensive studies on the interactions of metal complexes with helical DNA duplexes, there are relatively few related studies with secondary DNA structures.[12b,l−u] Herein we show that the Pt^{II} complexes **1**−**7** (Figure 1) bearing dppz or substituted dppz ligands bind to G-quadruplexes. The tightest binding was obtained from the water-soluble complex $[Pt^{II}(dppz\text{-}COOH)(N^\wedge C)]CF_3SO_3$ (**1**; dppz-COOH = 11-carboxydipyrido[3,2-*a*:2′,3′-*c*]phenazine, N^CH = 2-phenylpyridine), which binds to G-quadruplexes with an accompanying 293-fold increase in its photoluminescence at λ_{max} = 512 nm. Results from a biotinylated primer extension telomerase assay demonstrated that **1** inhibited human telomerase in vitro with a $^{tel}IC_{50}$ = 760 nM.

Results

The ligand dppz and its derivatives dppz-COOH, dppx (11,12-dimethyldipyrido[3,2-*a*:2′,3′-*c*]phenazine), dppc (11,12-dichlorodipyrido[3,2-*a*:2′,3′-*c*]phenazine), and dppp2 (pyrido[2′,3′:5,6]pyrazino[2,3-*f*][1,10]phenanthroline) used in this work were prepared according to the literature methods (see the Experimental Section). Treatment of these ligands with $Bu_4N[Pt(N^\wedge C)Cl_2]$ or $Bu_4N[Pt(Thpy)Cl_2]$ (Thpy = 2-(2′-thienyl)pyridine) in refluxing CH_3CN in the presence of $AgCF_3SO_3$ afforded **1**−**5** in 70−86% yields (Scheme S1 in the Supporting Information). The syntheses of **6** and **7** by reacting $[Pt(dppz)Cl_2]$ with 4-aminopyridine (NH_2py-4) or 1-methylimidazole (Meim-1) were reported previously.[15d]

Complexes **1**−**5** were characterized by ^{1}H NMR and UV−vis spectroscopy, mass spectrometry, and elemental analyses (see the Experimental Section and Table 1). These complexes are soluble at a concentration of 100 μM in CH_3CN or in Tris/KCl buffer (100 mM KCl, 10 mM Tris−HCl, pH 7.5) at room temperature and remain intact in Tris/KCl buffer for >72 h at room temperature (as revealed by both UV−vis absorption and NMR spectroscopy). The pK_a value of the COOH group in **1** was determined to be 3.2 by UV−vis spectrophotometry, suggesting that in the Tris/KCl buffer solution this complex exists as a zwitterionic, net charge neutral species containing a deprotonated carboxylate.

Spectroscopic Properties. The UV−vis absorption data of **1**−**5** are summarized in Table 1. Similar to the reported absorption spectral data of **6** and **7** in CH_3CN solutions,[15d] there is an intense absorption band at 320−390 nm, which is assigned to intraligand (IL) transition(s), and a broad absorption band at 410−447 nm. The λ_{max} of the absorption at 410−447 nm varies

(12) Examples of G-quadruplex-interactive telomerase inhibitors. Cationic porphyrins:(a) Wheelhouse, R. T.; Sun, D.; Han, H.; Han, F. X.; Hurley, L. H. *J. Am. Chem. Soc.* **1998**, *120*, 3261. (b) Shi, D.-F.; Wheelhouse, R. T.; Sun, D.; Hurley, L. H. *J. Med. Chem.* **2001**, *44*, 4509. Anthraquinones: (c) Sun, D.; Thompson, B.; Cathers, B. E.; Salazar, M.; Kerwin, S. M.; Trent, J. O.; Jenkins, T. C.; Neidle, S.; Hurley, L. H. *J. Med. Chem.* **1997**, *40*, 2113. Tricyclic or tetracyclic compounds: (d) Perry, P. J.; Read, M. A.; Davies, R. T.; Gowan, S. M.; Reszka, A. P.; Wood, A. A.; Kelland, L. R.; Neidle, S. *J. Med. Chem.* **1999**, *42*, 2679. (e) Perry, P. J.; Gowan, S. M.; Read, M. A.; Kelland, L. R.; Neidle, S. *Anti-Cancer Drug Des.* **1999**, *14*, 373. Perylenes: (f) Fedoroff, O. Y.; Salazar, M.; Han, H.; Chemeris, V. V.; Kerwin, S. M.; Hurley, L. H. *Biochemistry* **1998**, *37*, 12367. Ethidium and derivatives: (g) Guo, Q.; Lu, M.; Marky, L. A.; Kallenbach, N. R. *Biochemistry* **1992**, *31*, 2451. (h) Koeppel, F.; Riou, J.-F.; Laoui, A.; Mailliet, P.; Arimondo, P. B.; Labit, D.; Petitgenet, O.; Hélène, C.; Mergny, J.-L. *Nucleic Acids Res.* **2001**, *29*, 1087. Pentacyclic acridines: (i) Gowan, S. M.; Heald, R.; Stevens, M. F. G.; Kelland, L. R. *Mol. Pharmacol.* **2001**, *60*, 981. (j) Gowan, S. M.; Harrison, J. R.; Patterson, L.; Valenti, M.; Read, M. A.; Neidle, S.; Kelland, L. R. *Mol. Pharmcol.* **2002**, *61*, 1154. (k) Kim, M. Y.; Vankayalapati, H.; Shin-Ya, K.; Wierzba, K.; Hurley, L. H. *J. Am. Chem. Soc.* **2002**, *124*, 2098. Cisplatin and derivatives: (l) Redon, S.; Bombard, S.; Elizondo-Riojas, M. A.; Chottard, J. C. *Biochemistry* **2001**, *40*, 8463. Other metal compounds: (m) Tuntiwechapikul, W.; Salazar, M. *Biochemistry* **2001**, *40*, 13652. (n) Smirnov, I. V.; Kotch, F. W.; Pickering, I. J.; Davis, J. T.; Shafer, R. H. *Biochemistry* **2002**, *41*, 12133. (o) Reed, J. E.; Arnal, A. A.; Neidle, S.; Vilar, R. *J. Am. Chem. Soc.* **2006**, *128*, 5992. (p) Bertrand, H.; Bombard, S.; Monchaud, D.; Teulade-Fichou, M. P. *J. Biol. Inorg. Chem.* **2007**, *12*, 1003. (q) Evans, S. E.; Mendez, M. A.; Turner, K. B.; Keating, L. R.; Grimes, R. T.; Melchoir, S.; Szalai, V. A. *J. Biol. Inorg. Chem.* **2007**, *12*, 1235. (r) Bertrand, H.; Monchaud, D.; De Cian, A.; Guillot, R.; Mergny, J. L.; Teulade-Fichou, M. P. *Org. Biomol. Chem.* **2007**, *5*, 2555. (s) Dixon, I. M.; Lopez, F.; Tejera, A. M.; Esteve, J.-P.; Blasco, M. A.; Pratviel, G.; Meunier, B. *J. Am. Chem. Soc.* **2007**, *129*, 1502. (t) Shi, S.; Liu, J.; Yao, T.; Geng, X.; Jiang, L.; Yang, Q.; Cheng, L.; Ji, L. *Inorg. Chem.* **2008**, *47*, 2910. (u) Kieltyka, R.; Fakhoury, J.; Moitessier, N.; Sleiman, H. F. *Chem.—Eur. J.* **2008**, *14*, 1145. (v) Kieltyka, R.; Englebienne, P.; Fakhoury, J.; Autexier, C.; Moitessier, N.; Sleiman, H. F. *J. Am. Chem. Soc.* **2008**, *130*, 10040.

(13) Ishibashi, T.; Lippard, S. J. *Proc. Natl. Acad. Sci. U.S.A.* **1998**, *95*, 4219.

(14) Jamieson, E. R.; Lippard, S. J. *Chem. Rev.* **1999**, *99*, 2467.

(15) (a) Liu, H.-Q.; Peng, S.-M.; Che, C.-M. *J. Chem. Soc., Chem. Commun.* **1995**, 509. (b) Liu, H.-Q.; Cheung, T.-C.; Che, C.-M. *Chem. Commun.* **1996**, 1039. (c) Wu, L.-Z.; Cheung, T.-C.; Che, C.-M.; Cheung, K.-K.; Lam, M. H. W. *Chem. Commun.* **1998**, 1127. (d) Che, C.-M.; Yang, M.; Wong, K.-H.; Chan, H.-L.; Lam, W. *Chem.—Eur. J.* **1999**, *5*, 3350. (e) Chan, H.-L.; Ma, D.-L.; Yang, M.; Che, C.-M. *ChemBioChem* **2003**, *4*, 62. (f) Ma, D.-L.; Che, C.-M. *Chem.—Eur. J.* **2003**, *9*, 6133. (g) Ma, D.-L.; Shum, T. Y.-T.; Zhang, F.; Che, C.-M.; Yang, M. *Chem. Commun.* **2005**, 4675.

(16) For more examples of intercalation of square planar platinum complexes into double helical DNA, see:(a) Jennette, K. W.; Lippard, S. J.; Vassiliades, G. A.; Bauer, W. R. *Proc. Natl. Acad. Sci. U.S.A.* **1974**, *71*, 3839. (b) Sundquist, W. I.; Lippard, S. J. *Coord. Chem. Rev.* **1990**, *100*, 293.

(17) (a) Arena, G.; Monsa Scolaro, L.; Pasternack, R. F.; Romeo, R. *Inorg. Chem.* **1995**, *34*, 2994. (b) Cusumano, M.; Di Pietro, M. L.; Giannetto, A.; Nicolo, F.; Rotondo, E. *Inorg. Chem.* **1998**, *37*, 563. (c) Lu, W.; Vicic, D. A.; Barton, J. K. *Inorg. Chem.* **2005**, *44*, 7970.

(18) Howe-Grant, M.; Lippard, S. J. *Biochemistry* **1979**, *18*, 5762.

(19) Erkkila, K. E.; Odom, D. T.; Barton, J. K. *Chem. Rev.* **1999**, *99*, 2777.

(20) Lai, S.-W.; Che, C.-M. *Top. Curr. Chem.* **2004**, *241*, 27.

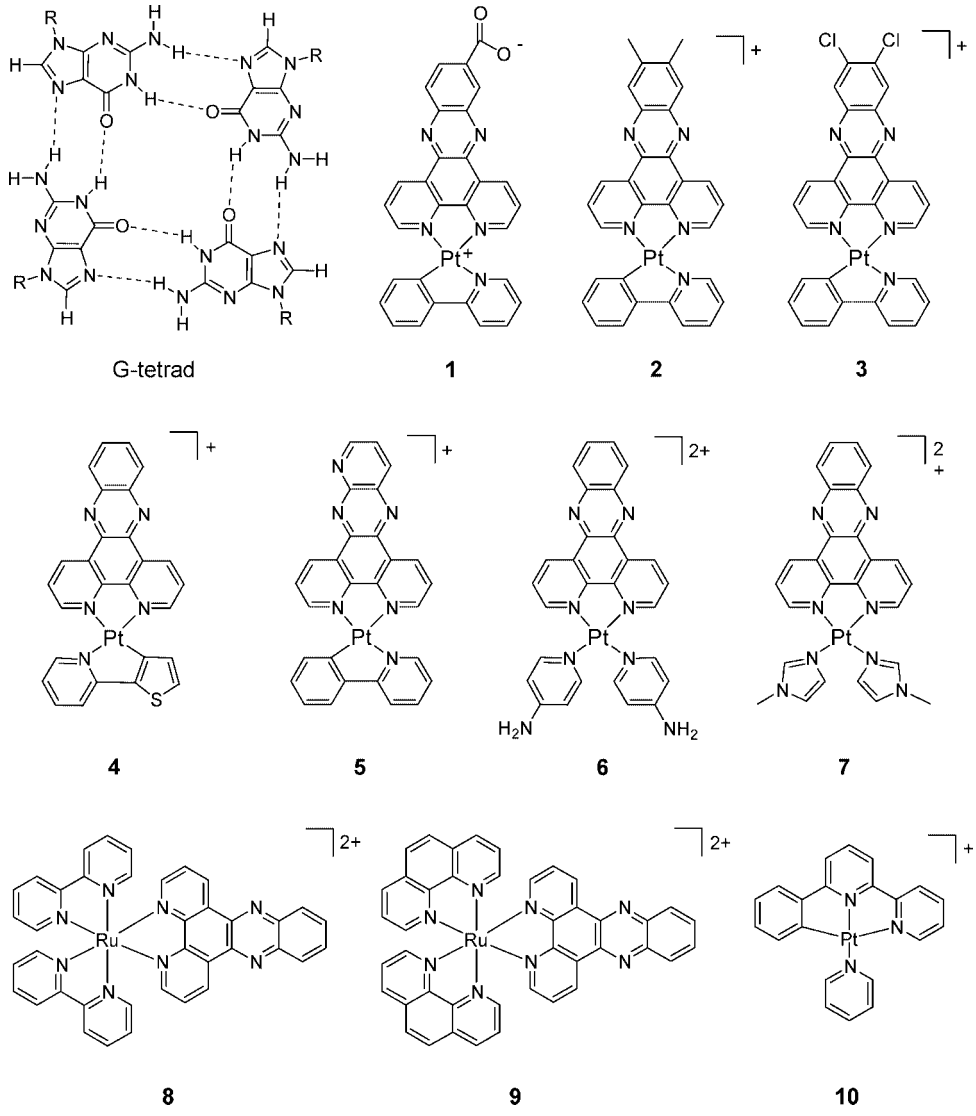

Figure 1. Schematic drawings of a guanine tetrad (G-tetrad) and complexes **1**−**10** (the zwitterionic, net charge neutral form of **1** was based on the pK_a value of 3.2 determined for its COOH group).

with the diimine ligands. As a similar absorption band is absent in $[Pt(en)(tN^{\wedge}C)]^+$ (en = 1,2-diaminoethane), the assignment of a (5d)Pt → $\pi^*(tN^{\wedge}C)$ transition is not favored. The absorption at 410−447 nm is assigned to a ^{1}MLCT (5d)Pt → π^*(dppz) transition. There is little solvent effect on the absorption spectra of **1**−**5**. As an example, the absorption λ_{max} of **1** in CH_3CN (321 nm) is similar to that in CH_2Cl_2 (324 nm), and the lower energy broad absorption at 410−447 nm remains relatively unchanged. The UV−vis absorption spectra of **1** (20 μM) in various solvents (Figure S1) and the UV−vis absorption data (Table S1) are given as Supporting Information. The profiles of the absorption spectra for **1**−**5** are similar to those of **6** and **7** recorded in CH_3CN solutions.

Excitation of **1** (27 μM in CH_3CN) at 350 nm gives an emission at 477 nm ($\phi = 0.01$, $\tau = 5.8$ μs). A similar emission at $\lambda_{max} \approx 475$ nm was found for complexes **2**, **3**, and **5** in CH_3CN solutions. There are only minor variations in the emission maxima [476 nm (**2**), 475 nm (**3**), 475 nm (**5**)] and lifetimes [7.0 μs (**2**), 2.4 μs (**3**), 2.8 μs (**5**)] among these three complexes. As the dppz ligands of **1**−**5** are different, we assign the 477 and 479 nm emissions of **1** in CH_3CN and CH_2Cl_2, respectively, to a $^3\pi\pi^*$ excited state of the C^N ligand. Similar to the absorption spectra, the emission spectra of **1**−**5** are minimally affected by solvents. For example, the emission λ_{max} of **1** slightly shifts from 477 nm in CH_3CN to 479 nm in CH_2Cl_2 (Figure S2, Supporting Information). In a frozen CH_3CN solution of **1** at 77 K, the emission λ_{max} occurs at 667 nm, which is similar to its solid-state emission ($\lambda_{max} = 674$ nm) at 298 K. The substantial red shift of these two emissions at 667 nm (frozen CH_3CN) and 674 nm (solid state) from that recorded in CH_3CN solution ($\lambda_{max} = 477$ nm) at room temperature indicates that the former two emissions come from electronic excited states different from the $^3\pi\pi^*$ excited state of the C^N ligand. According to previous work,[15d] $[Pt(dppz)(tN^{\wedge}C)]^+$ cations stack in the solid state with intermolecular Pt−Pt contacts of ca. 3.4 Å, which allows for platinum(II)−platinum(II)/ligand−ligand interactions. Therefore, the emissions with λ_{max} at 667 and 674 nm are assigned to the ^{3}MMLCT (metal−metal to ligand charge transfer) excited state.[15d] The photophysical data of **1**−**5** are given in Table S2, Supporting Information.

Gel Mobility Shift Assay. By employing a native PAGE assay, we examined the ability of the complexes to assemble intermolecular G-quadruplexes from the oligonucleotide TR2 [5′-TACAGATAG(TTAGGG)$_2$TTA-3′], which contains two tan-

Scheme 1. Sequences of Oligonucleotides TR2 and G4A1 and Possible Structures of Intermolecular Quadruplexes of TR2 and the Intramolecular G4A1-Quadruplex

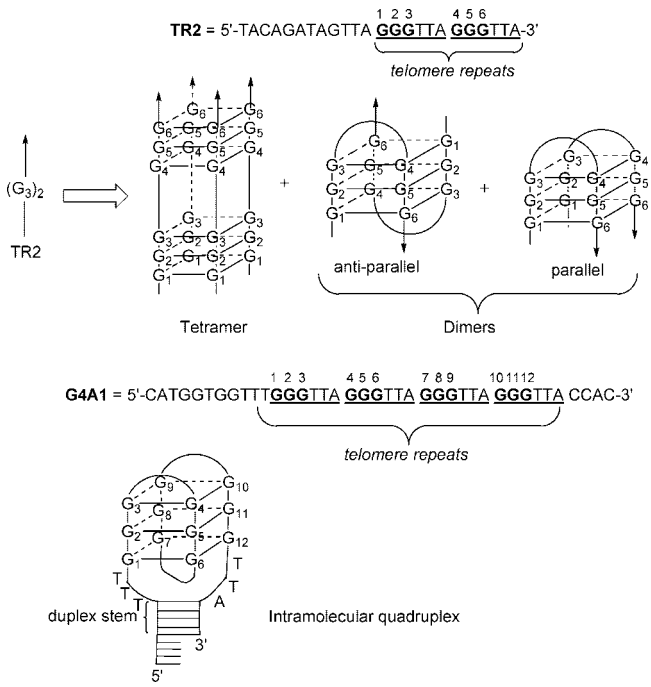

dem human telomeric sequences and can associate into antiparallel and parallel G-quadruplexes, in dimeric (D) and tetrameric (T) forms (Scheme 1).[21a,b] When the TR2 oligonucleotide was incubated in Tris buffer (10 mM Tris, 1 mM EDTA, 100 mM KCl, pH 8.0), gel mobility shift assays revealed that there was no formation of G-quadruplex structure and only the band corresponding to the monomer (M) could be observed. Adding **1**−**7** in increasing concentrations from 0.08 to 15 μM to a solution of TR2 oligonucleotide resulted in progressive appearance of new bands with reduced mobility, corresponding to the D and T G-quadruplex structures. These bands were not observed when oligonucleotide MTR2 [5′-TACAGATAGTTA-GACTTAACGTTA-3′] lacking three consecutive guanines was used. The best result was attained with **1**, which has the highest solubility in buffer solution. As depicted in Figure 2a, up to 32% of the TR2 oligonucleotide adopted a dimeric G-quadruplex upon addition of **1** at 0.6 μM. Complexes **2**−**7** have a lower solubility in Tris buffer, and a higher complex concentration (~6 μM) was required to achieve ~30% dimeric G-quadruplex formation (Figure 2b). Treatment of TR2 oligonucleotide with free dppz at concentrations from 3 to 24 μM failed to promote the formation of any significant amount of G-quadruplex structures (Figure S3, Supporting Information). Because the G-quadruplex formed from TR2 oligonucleotide is polymorphic, gel mobility shift assay using a well-characterized G-quadruplex structure formed from the oligonucleotide Telo21 [5′-GGG(T-TAGGG)$_3$-3′] was performed.[21c] The result revealed that **1** can also promote G-quadruplex formation from Telo21 oligonucleotide (for details, see Figure S4, Supporting Information).

Complexes **8**−**10** are known to bind to double-stranded DNA.[15f,22] Treatment of TR2 oligonucleotide (8 μM) with these

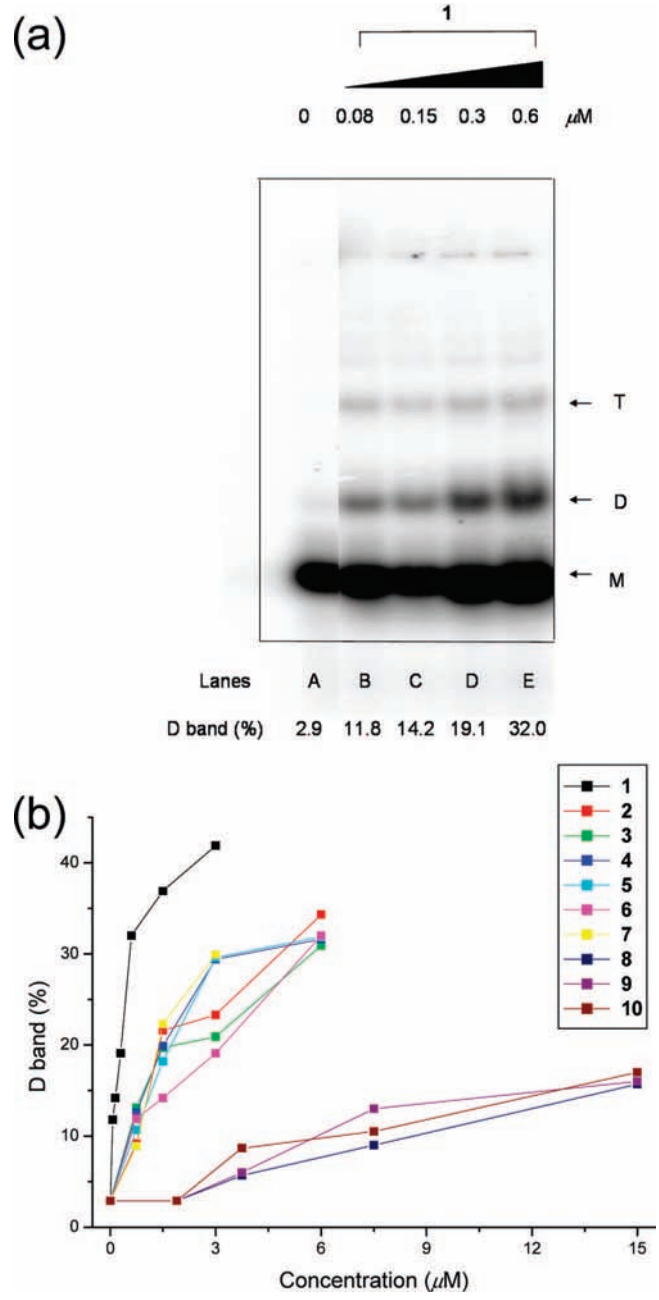

Figure 2. (a) Platinum(II) complex-assisted assembly of G-quadruplexes from oligonucleotide TR2 illustrated by native PAGE analysis. Platinum complexes at the indicated concentration were incubated with TR2 (8 μM) at 20 °C in a buffer containing 10 mM Tris, 1 mM EDTA, 100 mM KCl, pH 8.0. Major bands were identified as monomer (M), dimer (D), and tetramer (T) on the basis of related literature reports.[21] (b) Intensity of band D (%) vs concentration.

complexes at concentrations of 0.75−6 μM in Tris buffer afforded <10% G-quadruplexes, and only the monomer (M) was visible in the gel shift assay. However, when the complex concentration was increased to >15 μM, formation of the dimeric and tetrameric G-quadruplexes became detectable.

Absorption Titration. The reactions of **1**−**10** with a G-quadruplex were examined by UV−vis absorption titration

(21) (a) Han, H.; Cliff, C. L.; Hurley, L. H. *Biochemistry* **1999**, *38*, 6981. (b) Teulade-Fichou, M.-P.; Carrasco, C.; Guittat, L.; Bailly, C.; Alberti, P.; Mergny, J.-L.; David, A.; Lehn, J.-M.; Wilson, W. D. *J. Am. Chem. Soc.* **2003**, *125*, 4732. (c) Zhou, J.-L.; Lu, Y.-J.; Ou, T.-M.; Zhou, J.-M.; Huang, Z.-S.; Zhu, X.-F.; Du, C.-J.; Bu, X.-Z.; Ma, L.; Gu, L.-Q.; Li, Y.-M.; Chan, A. S.-C. *J. Med. Chem.* **2005**, *48*, 7315.

(22) (a) Friedman, A. E.; Chambron, J.-C.; Sauvage, J.-P.; Turro, N. J.; Barton, J. K. *J. Am. Chem. Soc.* **1990**, *112*, 4960. (b) Jenkins, Y.; Friedman, A. E.; Turro, N. J.; Barton, J. K. *Biochemistry* **1992**, *31*, 10809.

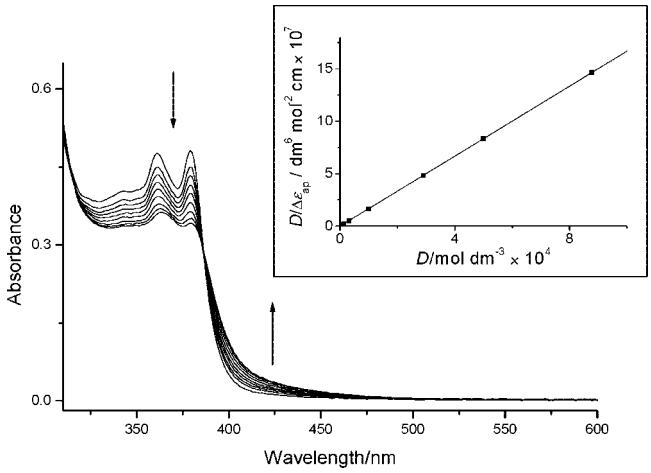

Figure 3. UV−vis spectra of **1** (50 μM) in Tris/KCl buffer (100 mM KCl, 10 mM Tris−HCl, pH 7.5) with increasing amounts of oligonucleotide G4A1 at 20.0 °C ([G4A1-quadruplex]/[Pt] = 0−20). Inset: $D/\Delta\varepsilon_{ap}$ vs D.

experiments. An intramolecular G-quadruplex was prepared by incubating oligonucleotide G4A1 [5′-CATGGTGGTTT-$(GGGTTA)_4$CCAC-3′] containing four human telomeric sequences in Tris/KCl buffer, which was heated to 95 °C for 10 min and then cooled to room temperature overnight.[23] The expected secondary DNA structure was confirmed by a positive CD peak at ∼290 nm and a negative CD peak at ∼240 nm (Figure S5, Supporting Information). As shown in Figure 3, addition of the G4A1-quadruplex to a solution of **1** in a Tris/KCl buffer at [G4A1-quadruplex]/[Pt] ratios ≥20/1 led to a 5 nm red shift and 30% hypochromism of the band at 362 nm. Isosbestic points were located at 313 and 386 nm. Analogous absorption titration reactions of the G4A1-quadruplex with **2**−**7**, at [G4A1-quadruplex]/[Pt] ratios >20/1 also revealed isosbestic spectral changes (Figures S6−S10, Supporting Information).

The spectral changes depicted in Figure 3 are not attributed to the binding of **1** to the unstructured form of the G4A1 oligonucleotide. Given that the N7 position of guanine is essential for G-quadruplex assembly by Hoogsteen-type hydrogen bonding, methylation of the N7 atom by dimethyl sulfate (DMS) disables the formation of the G4A1-quadruplex.[12h] After pretreatment of the G-quadruplex with DMS, a UV−vis absorption titration of the methylated oligonucleotide (G4A1-DMS) with **1** was undertaken. No significant spectral changes were observed at [G4A1-DMS]/[**1**] ratios >20/1 in Tris/KCl buffer at 20.0 °C. Similar findings were observed upon treatment of **1** with unstructured $(dT)_{26}$ oligonucleotide (5′-TTTTTTTTTTTTTTTTTTTTTTTTTT-3′) under the same reaction conditions.

DNA ligase assay was used to confirm the formation of a double-stranded stem region in the G4A1-quadruplex DNA (Figure S11, Supporting Information). Because this stem region in the G4A1-quadruplex contains five residues base-pairing via typical Watson/Crick-type interactions with their complementary bases, for stabilizing the G-quadruplex structure (Scheme 1), we cannot exclude the possibility of the interaction of the platinum(II) complex with the G4A1-quadruplex through this duplex region. To discount this possibility, we used a shorter oligonucleotide, G4A2 [5′-AGGG$(TTAGGG)_3$-3′], which has no duplex stem and is known to assemble into an intramolecular G-quadruplex in Tris/KCl buffer.[24] Treatment of **1** with the G4A2-quadruplex produced isosbestic spectral changes indicative of a binding interaction (see Figure S12, Supporting Information).

Derived from a plot of $D/\Delta\varepsilon_{ap}$ vs D according to the Scatchard equation (see the inset of Figure 3), the binding constants K under our experimental conditions (final concentration ≤5% DMF) at 20.0 °C for **1** with the G4A1- and G4A2-quadruplexes are $(9.7 \pm 1.1) \times 10^6$ and $(9.0 \pm 0.7) \times 10^6$ dm^3 mol^{-1}, respectively. The K values for **2** and **5**−**7** were similarly determined to be $\sim 10^6$ dm^3 mol^{-1} (see Table S3, Supporting Information). The K values for **3** and **4** could not be precisely determined due to their low solubility in buffer solutions. Notably, binding of these Pt(II) complexes to G-quadruplex DNA is favored at least 100-fold compared with that to nonquadruplex double-stranded DNA molecules consisting of complementary G4A1 oligonucleotide. The highest affinity and selectivity for G-quadruplex binding (up to ∼800-fold compared with those of nonquadruplex double-stranded DNA binding) was exhibited by **1**, which contains a COOH group at the periphery of the dppz ligand. The binding of $[Pt^{II}(C\hat{}N\hat{}N)(py)]ClO_4$ (**10**; HC^N^N = 6-phenyl-2,2′-bipyridine) to the G4A1-quadruplex has a smaller K value [$(2.0 \pm 0.9) \times 10^4$ dm^3 mol^{-1}] and shows no selectivity for the G-quadruplex vs typical double-stranded DNA. The two octahedral Ru−dppz complexes **8** and **9** were found to bind to the G-quadruplex with lower K values [$K = (5.8 \pm 0.6) \times 10^4$ dm^3 mol^{-1} (**8**) and $(6.3 \pm 0.3) \times 10^4$ dm^3 mol^{-1} (**9**)].

UV Melting Study. Additional evidence for G-quadruplex stabilization was provided by a thermal denaturating study. In the absence of any Pt(II) complex, the DNA melting temperature (T_m) of the G4A1-quadruplex in Tris/KCl buffer was 52 °C. However, upon treatment of the G4A1-quadruplex (20 μM) with an equimolar amount of the Pt-dppz complexes, a marked increase in T_m (10−14 °C) was registered. The highest T_m deviation [ΔT_m (change in DNA melting temperature) = 14 °C] was found with **1** (Figure S13, Supporting Information). This is consistent with the results of absorption titration studies that **1** has the highest K value [$(9.7 \pm 1.1) \times 10^6$ dm^3 mol^{-1}]. A comparison of the melting curves obtained for the G4A1-quadruplex in Tris/KCl and Tris/NaCl buffers (Figure S13, Supporting Information) revealed that the use of the same concentration of NaCl vs KCl in the buffer had no effect on the stem denaturation but significantly changed the quadruplex denaturation. The free dppz ligands did not cause a notable increase in the T_m of the G4A1-quadruplex.

Competition Dialysis. The binding affinity of **1** to different sequences of nucleic acids was evaluated by competition dialysis.[25] The results obtained in a 6 mM Na_2HPO_4, 2 mM NaH_2PO_4, 1 mM Na_2EDTA, 185 mM NaCl, pH 7.0, buffer[25b,c] are depicted in Figure 4, and those obtained in Tris/KCl buffer are shown in Figure S14 (Supporting Information). Complex **1** binds to G-quadruplexes derived from either G4A1 or G4A2 oligonucleotide, while no binding to single-stranded DNA (polydA) was observed. The affinity of **1** for double-stranded calf thymus DNA (ct DNA) is at least 10-fold lower than that for the G-quadruplex. A similar result was previously reported

(23) Han, F. X.; Wheelhouse, R. T.; Hurley, L. H. *J. Am. Chem. Soc.* **1999**, *121*, 3561.

(24) Wang, Y.; Patel, D. J. *Structure* **1993**, *1*, 263.

(25) (a) Müller, W.; Crothers, D. M. *Eur. J. Biochem.* **1975**, *54*, 267. (b) Ren, J.; Chaires, J. B. *Biochemistry* **1999**, *38*, 16067. (c) Heald, R. A.; Modi, C.; Cookson, J. C.; Hutchinson, I.; Laughton, C. A.; Gowan, S. M.; Kelland, L. R.; Stevens, M. F. G. *J. Med. Chem.* **2002**, *45*, 590.

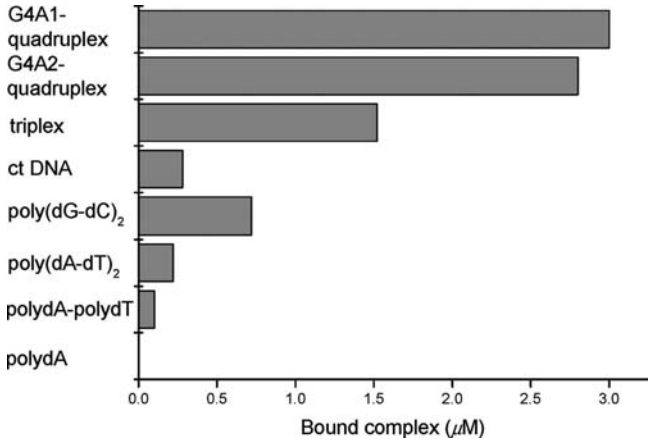

Figure 4. Competition dialysis assay. The amount of bound **1** to different sequences of nucleic acids is depicted as a bar chart. All measurements were performed in a 6 mM Na_2HPO_4, 2 mM NaH_2PO_4, 1 mM Na_2EDTA, 185 mM NaCl, pH 7.0, buffer.

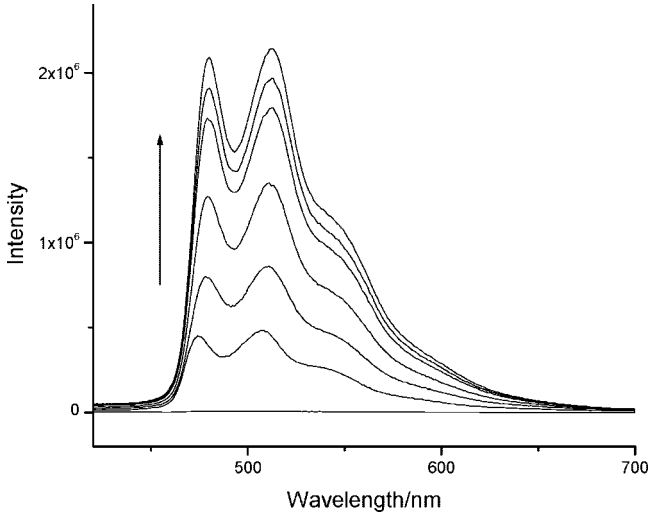

Figure 5. Emission spectral traces of **1** (50 μM) in Tris/KCl buffer (100 mM KCl, 10 mM Tris HCl, pH 7.5) with increasing ratios of [G4A1-quadruplex]/[Pt] = 0−20 at 20.0 °C.

for pentacyclic acridine RHPS4 (3,11-difluoro-6,8,13-trimethyl-8*H*-quino[4,3,2-*kl*]acridinium methosulfate), which was found to have a higher binding affinity (over 2-fold) for G-quadruplex DNA compared with double-stranded or single-stranded DNA, as measured by competition dialysis.[25c]

Emission Titration. Complex **1** (50 μM) is weakly emissive (λ_{max} = 477 nm) in aqueous Tris/KCl buffer solution at 20.0 °C (Figure S15, Supporting Information). Upon addition of the G4A1-quadruplex, an intense emission at λ_{max} = 512 nm developed (Figure 5). The emission intensity increased with the concentration of the G-quadruplex and saturated at a [G-quadruplex]/[**1**] ratio ≥20. As shown by a plot of I/I_o vs [G-quadruplex]/[**1**] (I and I_o are the emission intensities with and without the G-quadruplex, respectively), the emission intensity at 512 nm was enhanced by a factor of up to 293 (Figure 6). When a similar emission titration experiment was performed using nonquadruplex double-stranded DNA molecules consisting of complementary G4A1 oligonucleotide, the emission intensity at 512 nm was enhanced by a factor of 27. Similar studies of **1** with ct DNA, poly(dA-dT)$_2$, and poly(dG-dC)$_2$ individually gave an emission at λ_{max} = 512 nm, the intensity of which was enhanced by a factor of 6, 3, and 6,

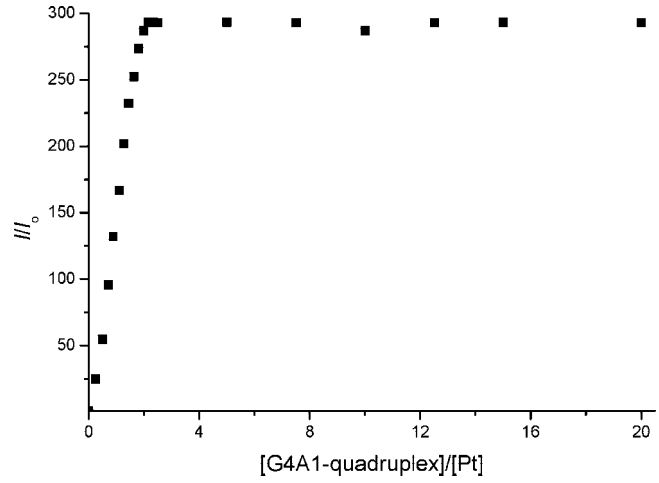

Figure 6. I/I_o vs [G4A1-quadruplex]/[Pt] for the emission titration study of **1** with the G4A1-quadruplex.

respectively (Figure S16, Supporting Information). The addition of an unstructured form of DNA [G4A1-DMS or the $(dT)_{26}$ oligonucleotide] to an aqueous Tris/KCl buffer solution of **1** at 20.0 °C did not increase the emission intensity, revealing that the 293-fold emission enhancement for the reaction of **1** with the G-quadruplex is not the result of binding to the unstructured form of DNA. Complexes **2**−**5** have a lower solubility than **1** in buffer solutions, and a less than 25-fold enhancement in emission intensity at $\lambda_{max} \approx$ 510 nm was recorded for similar emission titration studies of these complexes with the G4A1-quadruplex. For **6** or **7**, no photoluminescence was observed in solutions or the solid state, and no enhancement in emission intensity was recorded for a similar emission titration study with the G4A1-quadruplex.

Detection of G-Quadruplex DNA in PAGE. Complex **1** was examined as a gel staining reagent for G-quadruplex DNA after electrophoresis on native polyacrylamide gels. Aliquots of a stock DNA solution (10 μM) for PAGE were added to a final volume of 20 μL for each lane. The detection of G-quadruplex DNA (Telo21) at concentrations of 0.5−4.0 μM was conducted by electrophoresis on polyacrylamide gel and subsequent staining with **1** for 30 min. As shown in Figure 7, incubating the polyacrylamide gel in a solution of **1** (1.5 mg/20 mL) for 30 min resulted in progressive appearance of a band corresponding to the G-quadruplex DNA. These results indicate that G-quadruplex DNA in micromolar concentration could be detected upon irradiation with long-wavelength UV in the presence of **1**. In contrast, **1** only weakly stained the double-stranded DNA consisting of complementary Telo21 oligonucleotide (Figure 7).

NMR Experiments. To elucidate the binding mode of **1**, we conducted a number of ^{1}H NMR experiments in phosphate buffer (90% H_2O/10% D_2O with 150 mM KCl, 25 mM KH_2PO_4, and 1 mM EDTA, pH 7.0). An intramolecular G4A4-quadruplex[26] and an intermolecular G4A3-quadruplex,[27] both with clearly assigned G-tetrad imino proton signals in the literature, were used for these studies. Upon addition of **1** to a solution of

(26) Phan, A. T.; Kuryavyi, V.; Gaw, H. Y.; Patel, D. J. *Nat. Chem. Biol.* **2005**, *1*, 167.
(27) (a) Duan, W.; Rangan, A.; Vankayalapati, H.; Kim, M.-Y.; Zeng, Q.; Sun, D.; Han, H.; Fedoroff, O. Y.; Nishioka, D.; Rha, S. Y.; Izbicka, E.; Von Hoff, D. D.; Hurley, L. H. *Mol. Cancer Ther.* **2001**, *1*, 103. (b) Kern, J. T.; Thomas, P. W.; Kerwin, S. M. *Biochemistry* **2002**, *41*, 11379.

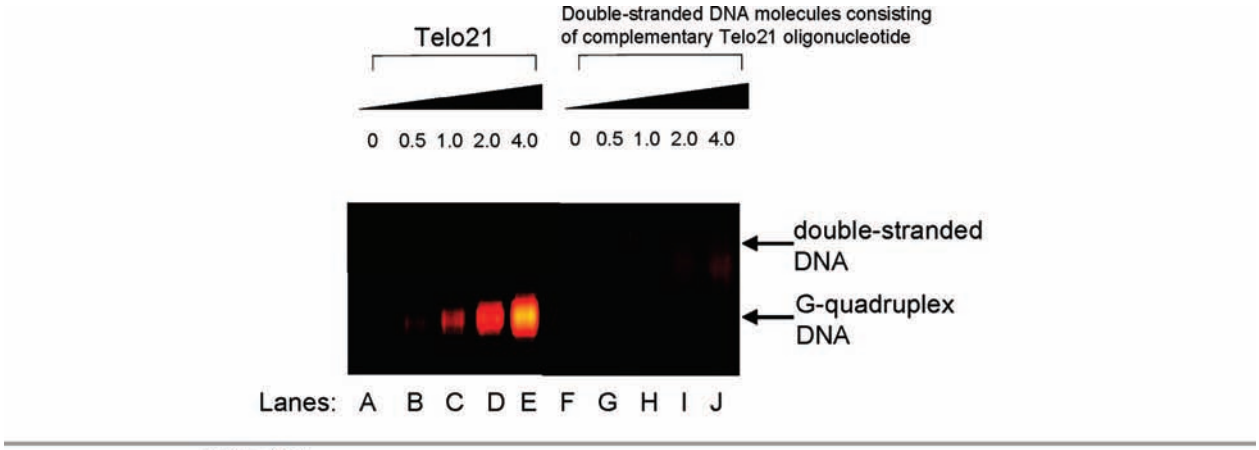

	Volume (μL)									
	Lane A	Lane B	Lane C	Lane D	Lane E	Lane F	Lane G	Lane H	Lane I	Lane J
Stock DNA solution (10 μM)	0	1	2	4	8	0	1	2	4	8
DI H_2O	20	19	18	16	12	20	19	18	16	12
Total	20	20	20	20	20	20	20	20	20	20

Figure 7. (a) Emissive PAGE analysis of G-quadruplex DNA (formed from Telo21 oligonucleotide) and double-stranded DNA molecules consisting of complementary Telo21 oligonucleotide upon staining with complex **1** (1.5 mg/20 mL, staining time 30 min). Aliquots of a stock DNA solution (10 μM) for PAGE were added to a final volume of 20 μL for each lane. Lanes A−E: 0, 0.5, 1.0, 2.0, and 4.0 μM G-quadruplex DNA per lane, respectively. Lanes F−J: 0, 0.5, 1.0, 2.0, and 4.0 μM double-stranded DNA per lane, respectively.

Scheme 2. Interaction of **1** with G-Quadruplex DNA

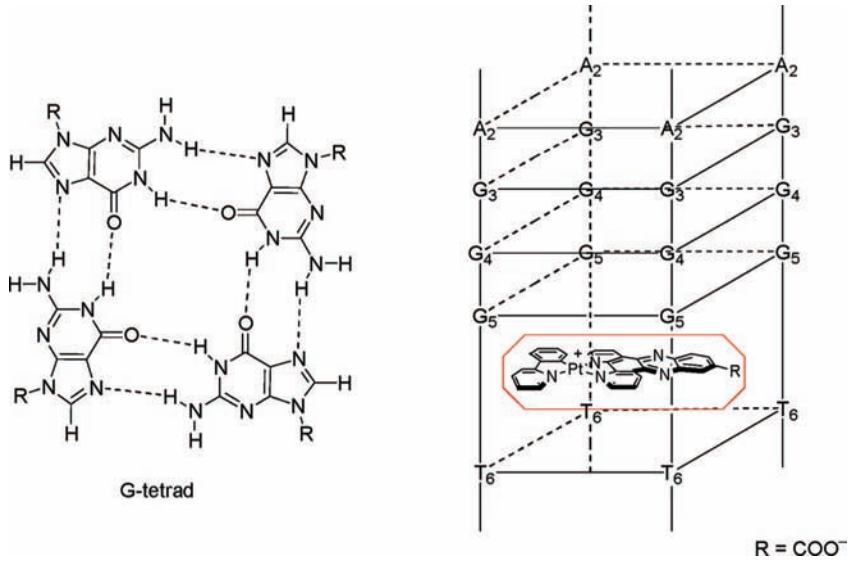

the G4A4-quadruplex (1.0 mM) at a [**1**]/[G4A4-quadruplex] ratio of 0.5/1, the imino proton resonances of the residues in the G-tetrad were shifted upfield and broadened, without being separated into two sets that correspond to the free and bound G4A4-quadruplex (Figure S17, Supporting Information). This could be attributed to the stacking of **1** on the G-tetrad, coupled with an exchange at an intermediate rate on the NMR time scale between the G4A4-quadruplex molecules with and without binding **1**. Increasing the [**1**]/[G4A4-quadruplex] ratio to 1/1 rendered the imino proton signals too broad to be detected. These observations preclude a clear assignment of the imino proton signals, by 2D NMR studies, for the spectra measured after addition of **1**.

The G4A3-quadruplex was prepared from a shorter oligonucleotide, G4A3 (5′-TAGGGTTA-3′); formation of the G4A3-quadruplex from this oligonucleotide was confirmed by gel electrophoresis. The ^{1}H NMR spectra recorded for the titration of the G4A3-quadruplex (1.0 mM) with **1** at various [**1**]/[G4A3-quadruplex] ratios are depicted in Figure 8. A 2D NOESY spectrum at a [**1**]/[G4A3-quadruplex] ratio of 1/1 is shown in Figure S18 (Supporting Information). The numbering of the residues, starting at the 5′ end of the DNA sequence, is T1, A2, G3, G4, G5, T6, T7, and A8. As depicted in Figure 8, addition of **1** caused a significant peak broadening and a large change in the chemical shifts of the imino protons, with the G3, G4, and G5 imino proton signals being upfield shifted by

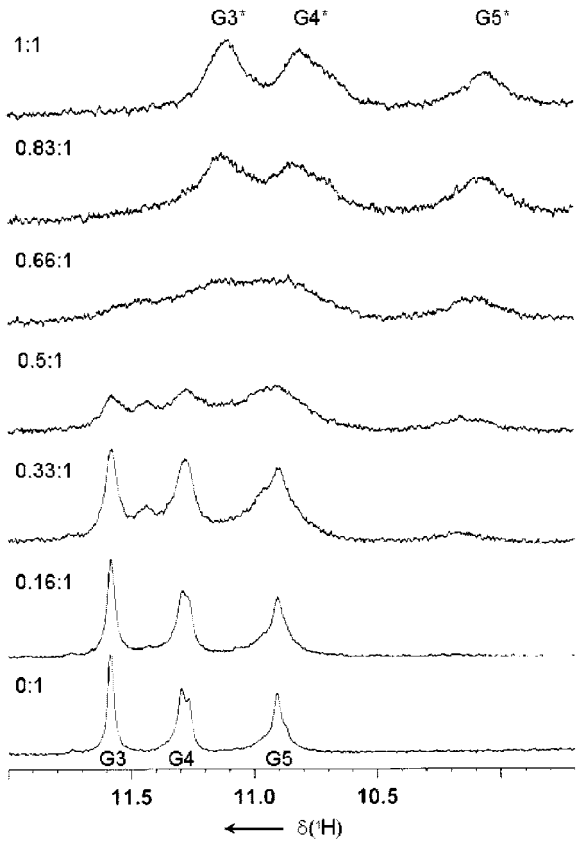

Figure 8. NMR titration of the G4A3-quadruplex with **1** at various [**1**]/[G4A3-quadruplex] ratios in 90% H_2O/10% D_2O with 150 mM KCl, 25 mM KH_2PO_4, 1 mM EDTA (pH 7.0). Only the imino proton signals (500 MHz, 27 °C) are shown.

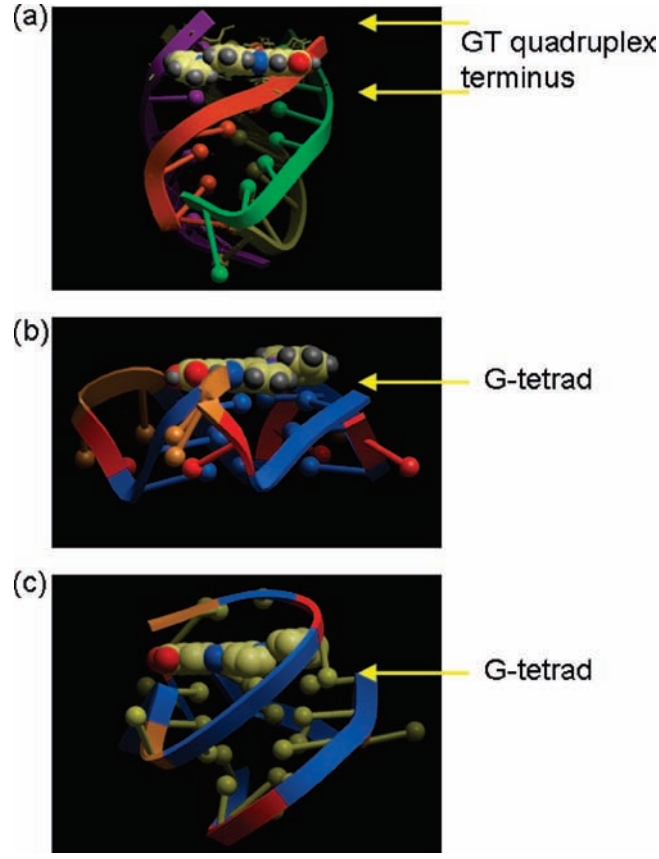

Figure 9. Molecular modeling of the binding interaction between **1** and (a) intermolecular G-quadruplex DNA $d(T_2AG_3T)_4$, (b) the human intramolecular telomeric repeat G4A2-quadruplex, and (c) the intramolecular telomeric G4A4-quadruplex.

0.53, 0.49, and 0.80 ppm, respectively, at a [**1**]/[G4A3-quadruplex] ratio of 1/1. The broadening of the imino proton signals could be due to an exchange at an intermediate rate on the NMR time scale between the G4A3-quadruplex molecules with and without binding **1**, and/or the multiple stacking configurations on the top of the G-tetrad.[26] At a [**1**]/[G4A3-quadruplex] ratio of 1.0, the G5 imino proton signal experienced the largest shift, suggesting that **1** binds close to the 3′ terminal face of the G-quadruplex DNA. The changes in chemical shifts are nearly identical to those exhibited by PIPER [*N*,*N*′-bis(2-(1-piperidino)ethyl)-3,4,9,10-perylenetetracarboxylic acid diimide] and *N*,*N*′-bis(3-(4-morpholino)propyl)-3,4,9,10-perylenetetracarboxylic acid diimide], both of which are known to bind to a G-quadruplex.[12f,27] We favor the model where **1** externally binds to the stacks of guanine quartets within a quadruplex, rather than intercalating between the stacks (Scheme 2).

Molecular Modeling. To provide insight into the binding mode(s), molecular modeling studies of the binding of **1** with intermolecular G-quadruplex $d(T_2AG_3T)_4$ and intramolecular G4A2- and G4A4-quadruplexes were performed. The results are given in Table S4 (Supporting Information). For $d(T_2AG_3T)_4$, the modeling study reveals that **1** binds to the four stranded parallel G-quadruplexes with a calculated binding energy of −54.00 kcal/mol (Figure 9a) and is stacked on the ends of the G-quadruplex at the GT-quadruplex terminus, close to the 3′ terminal face of the G-quadruplex. This is consistent with the model derived from the results of NMR experiments described in the previous section. In the case of intramolecular G-quadruplexes, the result reveals that **1** binds to the human intramolecular telomeric repeat G4A2-quadruplex with a calculated binding energy of −63.79 kcal/mol (Figure 9b) and is stacked on the ends of the G-quadruplex. A similar result was obtained for the intramolecular telomeric G4A4-quadruplex (Figure 9c), for which the calculated binding energy is −64.65 kcal/mol, with **1** being stacked on the ends of the G-quadruplex at the GT-quadruplex terminus, close to the 3′ terminal face of the G-quadruplex. In all three cases, the unfavorable binding energies of 20.60−72.63 kcal mol^{-1} calculated for the intercalation binding sites suggest that the interactions between **1** and G-quadruplex DNA should not be intercalative in nature.

Assay of Telomerase Activity. The inhibition of telomerase activities in HeLa-cell-free extracts was evaluated using a primer extension assay.[28] A 5′-biotinylated primer consisting of three telomeric repeats was used, and the incorporation of ^{32}P-labeled GTP was measured.[28] The inhibition experiments were performed with concentrations of the platinum(II)−dppz complexes fixed at 2.5 μM, and with 5,10,15,20-tetrakis(*N*-methyl-4-pyridyl)porphyrin (TMPyP4) as a positive control.[12a,b] As depicted in Figure 10, **1** exhibited the highest telomerase inhibitor effect. By measuring the inhibition of telomerase activities, the cell-free telomerase $^{tel}IC_{50}$ value (metal complex concentration that inhibited 50% of the telomerase activity vs a drug-free control) of **1** was determined to be 760 nM. Almost

(28) Sun, D.; Hurley, L. H.; Von Hoff, D. D. *BioTechniques* **1998**, *25*, 1046.
(29) (a) Haider, S. M.; Parkinson, G. N.; Neidle, S. *J. Mol. Biol.* **2003**, *326*, 117. (b) Read, M. A.; Neidle, S. *Biochemistry* **2000**, *39*, 13422.

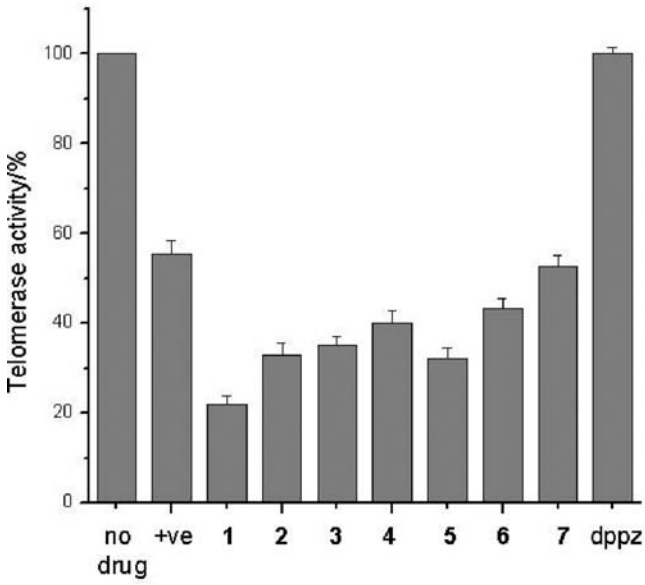

Figure 10. Cell-free inhibition of telomerase activity by platinum(II) complexes (2.5 μM). The average values from three independent experiments are shown, and error bars represent the standard deviation.

complete telomerase inhibition (~90%) was observed at [**1**] = 6 μM (Figure S19, Supporting Information). This $^{tel}IC_{50}$ value is comparable to those of previously reported G-quadruplex-interacting compounds such as acridine derivatives, ethidium derivatives, and quinolines, which have $^{tel}IC_{50}$ values of ca.100−500 nM.[12] Recently, molecules such as 9-anilinoproflavine, triazines, fluoroquinophenoxazines, telomestatin, and pentacyclic acridines with higher potency ($^{tel}IC_{50}$ of ca.5−100 nM), better selectivity, and higher binding affinity toward G-quadruplex DNA than duplex DNA have been reported.[12]

Cytotoxicity Test (MTT Assay). Using an MTT assay, the in vitro cytotoxicities of **1**−**7** against KB-3-1, KB-V1, HeLa, CNE1, and SUNE1 cancer cell lines were determined, and their toxicity to normal cells was evaluated using the CCD-19Lu (normal lung fibroblast) cell line. To summarize the findings, complex **1** is moderately cytotoxic with an IC_{50} value of 17−25 μM. It is potent against the multi-drug- and cisplatin-resistant KB-V-1 and CNE1 cell lines, with the resistance ratios being 1.2 and 1.1, respectively. Most importantly, it is ~10 times less cytotoxic (IC_{50} = 180 μM) to normal lung fibroblast cells. Details of the results are given in the Supporting Information (Table S5).

Discussion

G-quadruplex DNA is known to regulate telomerase activities. Therefore, inhibition of telomerase by inducing/stabilizing G-quadruplex formation is a strategy to design new anticancer drugs.[1−5,10,11] In the literature, there are already neutral and cationic planar organic compounds reported to bind to and stabilize G-quadruplexes, resulting in antitelomerase activity. Cationic Pt^{II} complexes containing extended π-conjugated dppz ligands constitute an interesting class of cationic planar metal−organic complexes. They structurally resemble other planar organic G-quadruplex binding molecules, but are different from those reported thus far in that they are phosphorescent molecules.

Molecular Light Switch Effect. Although there are reported telomerase inhibitors with high binding selectivity and affinity toward G-quadruplexes, emission spectroscopy (which is a sensitive bioanalytical tool) has seldom been used to examine the binding of these inhibitors to G-quadruplex DNA.

The Pt−dppz complex **1** is weakly emissive in aqueous buffer; its photoluminescence is significantly enhanced upon binding to G-quadruplex DNA, with up to 293-fold enhancement of emission intensity at 512 nm recorded at [G-quadruplex]/[**1**] ratios ≥20/1. The emission of the "**1** + G-quadruplex DNA" adduct at 512 nm is not the $^3\pi\pi^*$ emission of the C^N ligand, which occurs at a λ_{max} of 477 nm. We assign the 512 nm emission as originating from the ^{3}[Pt → π^*(dppz)] ^{3}MLCT excited state. As external end-stacking binding of the [Pt(dppz)] moiety of **1** to G-quadruplex DNA could result in the shielding of the hydrophobic [Pt(dppz)] unit from aqueous buffer solution, the nonradiative decay of the excited state via complex−solvent interaction could be suppressed.

Complex **1** can stain G-quadruplex DNA on native polyacrylamide gels, giving emissive gel images. G-quadrupelx DNA in micromolar concentration could be observed upon irradiation with long-wavelength UV in the presence of **1**, revealing a potential application of **1** in luminescent signaling of G-quadruplex DNA.

Specificity for G-Quadruplex DNA. Complexes **1**−**7** promote the assembly of intermolecular G-quadruplexes from the oligonucleotide TR2, and among these complexes, **1** promoted the formation of G-quadruplexes to the greatest extent. Even at 0.6 μM, up to 30% of TR2 oligonucleotide was converted to the dimeric G-quadruplex form. The cationic planar [Pt−dppz] motif is a key structural feature since treatment of TR2 oligonucleotide with octahedral complexes **8** and **9** (which also contain dppz ligands) at similar complex concentrations (0.75−6 μM) did not afford a significant amount of G-quadruplexes.

Thermal denaturing studies supported a mechanism involving intramolecular G-quadruplex stabilization. The induced stabilization of the G-quadruplexes was found to correlate with the telomerase inhibition activity. For **1**−**7**, over 50% telomerase inhibition was observed at [Pt] = 2.5 μM, which is consistent with the marked increase in T_m (by 10−14 °C) found for these complexes in thermal denaturing studies.

By comparing the K values, **1** has a nearly 800-fold higher binding affinity toward intramolecular G-quadruplex DNA from oligonucleotide G4A1 than for nonquadruplex double-stranded DNA molecules consisting of complementary G4A1 oligonucleotide. On the basis of the results of competition dialysis experiments, **1** was found to have a strong preference for binding to G-quadruplexes that were derived from either G4A1 or G4A2 oligonucleotides, while no binding to single-stranded DNA (polydA) was observed. In the literature, 3,6,9-trisubstituted acridine 9-[4-(*N*,*N*-dimethylamino)phenylamino]-3,6-bis(3-pyrrolodinopropionamido)acridine (BRACO19) was shown to have a higher binding affinity toward G-quadruplex DNA than double-stranded DNA, with a 25-fold difference in K values only.

Binding of 1 to G-Quadruplex DNA via an External End-Stacking Mode. On the basis of the NMR titration of the intermolecular G4A3-quadruplex with **1**, we propose that **1** binds to this G-quadruplex and is stacked on the ends of the G-quadruplex at the GT-quadruplex terminus, which is close to the 3′ terminal face of the G-quadruplex. This proposed model is supported by molecular modeling study of the binding interactions between **1** and intermolecular or intramolecular G-quadruplex DNAs [with favorable calculated binding energy −54.00 kcal/mol (intermolecular G-quadruplex) and −63.79 and −64.65 kcal/mol (intramolecular G-quadruplexes)]. A similar

external end-stacking binding mode has also been reported in a recent crystal-structure analysis of disubstituted acridine derivatives and the dimeric *Oxytricha* quadruplex.[29a] Neidle and co-workers had reported X-ray fiber diffraction data of the cocomplex formed by interaction of 1,4-disubstituted amidoanthraquinone (BSU-1071) with a synthetic $[d(TGGGT)]_4$ sequence, revealing an external end-stacking binding mode.[29b]

Nanomolar Potency against Telomerase. The first generation of G-quadruplex-interacting compounds such as anthraquinones, cationic porphyrins, fluorenones, and acridines have $^{tel}IC_{50}$ values in the micromolar range and a lower selectivity for G-quadruplexes vs other forms of DNA (e.g., the bisubstituted acridine compound BSU-6048, which has a 0.9-fold selectivity). Recent developments led to some potent G-quadruplex-interacting compounds ($^{tel}IC_{50}$ of ca.100−500 nM) based on ethidium, dibenzophenanthrolines, and pentacyclic acridine structures. The most potent G-quadruplex-interacting compound reported so far is telomestatin, a natural product, with a $^{tel}IC_{50}$ value of 5 nM.[12k]

Hurley and co-workers had described some metal−porphyrin complexes that are telomerase inhibitors, with activities comparable to those of free porphyrin ligands.[12b] For example, the planar complex Pt^{II}−TMPyP4 exhibited 69% inhibition and the Cu^{II}−TMPyP4 complex exhibited 75% inhibition at 25 μM.[12b] The Pt−dppz complexes described in this work are cationic planar molecules that contain an extended π-conjugated ligand. The Pt^{II} ion is needed for the G-quadruplex binding as the dppz ligand alone does not bind to G-quadruplex DNA nor promote the formation of intermolecular G-quadruplexes, according to the results of gel mobility shift assays, thermal denaturating studies, and antitelomerase assays. It is likely that the cationic charge of the Pt^{II} ion contributes to the high binding selectivity and affinity ($\sim 10^7$ dm^3 mol^{-1}) toward G-quadruplexes and the nanomolar potency against telomerase ($^{tel}IC_{50}$ = 760 nM). Indeed, the antitelomerase activity ($^{tel}IC_{50}$ = 760 nM) of **1** is comparable to those of some of the most potent G-quadruplex-interacting compounds reported in the literature [acridine derivatives, ethidium derivatives, quinolines ($^{tel}IC_{50}$ of ca.100−500 nM)].[12,30]

A high selectivity for G-quadruplex DNA over other forms of DNA and low cytotoxicities are essential properties for any G-quadruplex-interacting compounds for use as telomerase inhibitors or as probes for in vivo detection of G-quadruplex DNA. According to the selectivity index (SI; $IC_{50}/^{tel}IC_{50}$), **1** has a favorable selectivity profile (SI = 23), though the SI value is slightly lower than 40 for the pentacyclic acridine RHPS4. However, with this selectivity index value, it is possible to effectively inhibit telomerase activity with this class of G-quadruplex-interacting Pt^{II} complexes at concentrations that do not have a significant and general toxic effect upon normal cells. We used an MTT assay to determine whether the Pt−dppz complexes exhibited differential toxicity between tumor and normal cells. The results indicated that **1** was 10-fold less cytotoxic (IC_{50} = 180 μM) to normal lung fibroblast cells.

Conclusion

Molecules that bind to G-quadruplex DNA are usually cationically charged and have a large flat aromatic surface capable of π-stacking interactions. In this work, seven Pt−dppz complexes were prepared and assayed for telomerase inhibition and G-quadruplex binding activity. Complex **1** contains a dppz ligand with a pendant COOH functional group, which may be involved in H-bonding interaction with the guanine in the external tetrad of G-quadruplex DNA. This may account for the high binding selectivity and affinity ($\sim 10^7$ dm^3 mol^{-1}) of this complex toward the G-quadruplex, as well as its nanomolar potency against telomerase ($^{tel}IC_{50}$ = 760 nM).

We found that there is a significant molecular light switch effect upon binding of **1** with the G-quadruplex. The 293-fold increase in the emission intensity is encouraging and suggests that, with judicious choice of auxiliary ligands, phosphorescent platinum(II) complexes could be developed for luminescent signaling studies of secondary DNA structure.

Experimental Section

Materials. ct DNA, poly(dG-dC)$_2$, poly(dA-dT)$_2$, polydA-polydT, polydA-(polydT)$_2$, and polydA were purchased from Sigma Chemical Co. Ltd. DNA oligomers (G4A1 = 5′-CATGGTGGTTTGGGTTAGGGTTAGGGTTAGGGTTACCAC-3′, G4A2 = 5′-AGGGTTAGGGTTAGGGTTAGGG-3′, G4A3 = 5′-TAGGGTTA-3′, G4A4 = 5′- TGAGGGTGGIGAGGGTGGGGAAGG-3′, $(dT)_{26}$ = 5′-TTTTTTTTTTTTTTTTTTTTTTTTTT-3′, TR2 = 5′-TACAGATAGTTAGGGTTAGGGTTA-3′, MTR2 = 5′-TACAGATAGTTAGACTTAACGTTA-3′, Telo21 = 5′-GGGTTAGGGTTAGGGTTAGGG-3′, and 5′-biotinylated $(TTAGGG)_3$ primer) were obtained from GENSET Singapore Biotechnology Ltd. The DNA concentration per base pair was determined on the basis of the absorbance value at the indicated wavelength (ε_{260} = 13 200 M (strand)$^{-1}$ cm^{-1} for ct DNA, ε_{254} = 16 800 M (strand)$^{-1}$ cm^{-1} for poly(dG-dC)$_2$, ε_{260} = 12 000 M (strand)$^{-1}$ cm^{-1} for poly(dA-dT)$_2$, ε_{260} = 12 000 M (strand)$^{-1}$ cm^{-1} for polydA-polydT, ε_{257} = 8600 M (strand)$^{-1}$ cm^{-1} for polydA) using UV−vis absorption spectroscopy.[31] Unless otherwise stated, spectroscopic titration experiments were performed in Tris/KCl buffer (100 mM KCl, 10 mM Tris−HCl, pH 7.5).

The substituted *o*-diaminobenzene compounds Thpy and N^CH were obtained from Aldrich. The ligands dppz,[32] dppx,[33a] dppc,[33b] dppz-COOH,[33a] and dppp2[33a] and metal complexes $Bu_4N[Pt(N^C)Cl_2]$,[34] $Bu_4N[Pt(Thpy)Cl_2]$,[34] $[Pt(dppz)Cl_2]$,[35] $[Ru(bpy)_2Cl_2]$, $[Ru(phen)_2Cl_2]$, $[Pt(dppz)(NH_2py\text{-}4)_2](CF_3SO_3)_2$ (**6**),[15d] $[Pt(dppz)(Meim\text{-}1)_2](CF_3SO_3)_2$ (**7**),[15d] $[Ru(dppz)(bpy)_2](CF_3SO_3)_2$ (**8**),[36] $[Ru(dppz)(phen)_2](CF_3SO_3)_2$ (**9**),[33] and $[Pt^{II}(C^N^N)(py)]ClO_4$ (**10**)[15f] were prepared according to published methods. Stock solutions (10 mM) of metal complexes for titration studies were prepared in either DMSO or MeCN and diluted with deionized water. All the stock solutions were kept at −20 °C in the dark between experiments.

The parental epidermal carcinoma KB-3-1 cell line and the multidrug-resistant KB-V-1 variant (derived from KB-3-1 cells through a series of stepwise selections with vinblastin) were provided by Dr. Michael Gottesman, National Institutes of Health, Bethesda, MD. KB-V-1 cells were maintained in the presence of 1 μg/mL vinblastin. The SUNE1 cell line was derived from poorly differentiated NPC in Chinese patients. CCD-19Lu (normal lung fibroblast) and HeLa (human cervix epitheloid carcinoma) cells were obtained from the American Type Culture Collection. Cell proliferation kit I (MTT) from Roche was used for cytotoxicity evaluation.

Physical Measurements. Absorption spectra were recorded on a Perkin-Elmer Lambda 19 UV−vis spectrophotometer. Emission

(30) Cuesta, J.; Read, M. A.; Neidle, S. *Mini-Rev. Med. Chem.* **2003**, *3*, 11.
(31) Felsenfeld, G.; Hirschman, S. Z. *J. Mol. Biol.* **1965**, *13*, 407.
(32) Yamada, M.; Tanaka, Y.; Yoshimoto, Y.; Kuroda, S.; Shimao, I. *Bull. Chem. Soc. Jpn.* **1992**, *65*, 1006.
(33) (a) Hartshorn, R. M.; Barton, J. K. *J. Am. Chem. Soc.* **1992**, *114*, 5919. (b) Waterland, M. R.; Gordon, K. C.; McGarvey, J. J.; Jayaweera, P. M. *J. Chem. Soc., Dalton Trans.* **1998**, 609.
(34) Kvam, P. I.; Songstad, J. *Acta Chem. Scand.* **1995**, *49*, 313.
(35) Kato, M.; Kosuge, C.; Yano, S.; Kimura, M. *Acta Crystallogr., Sect. C* **1998**, *54*, 621.
(36) (a) Chambron, J.-C.; Sauvage, J.-P.; Amouyal, E.; Koffi, P. *New J. Chem.* **1985**, *9*, 527. (b) Amouyal, E.; Homsi, A.; Chambron, J.-C.; Sauvage, J.-P. *J. Chem. Soc., Dalton Trans.* **1990**, 1841.

spectra were recorded on a SPEX Fluorolog-2 model fluorescence spectrophotometer. UV melting studies were performed using a Perkin-Elmer Lambda 900 UV−vis spectrophotometer equipped with a Peltier temperature programmer, PTP-6. Positive ion FAB mass spectra were recorded on a Finnigan MAT95 mass spectrometer. Circular dichroism spectra were recorded on a JASCO J-810 spectropolarimeter equipped with a Peltier temperature control device.

Determination of the pK_a Value. Aliquot solutions of **1** at pH values of 1−10 were prepared. The molar extinction coefficient of each solution was determined at two wavelengths at which ε showed a change on going from acidic to basic solution. The pK_a value was determined graphically from the plots of ε values against the pH.

Gel Mobility Shift Assay.[12h] ^{32}P-labeled TR2 oligonucleotide at a concentration of 8 μM was annealed by heating in a 10 mM Tris/1 mM EDTA buffer containing 100 mM KCl (pH 8.0) to 95 °C for 10 min followed by cooling to room temperature. A stock solution (2 μL) of the metal complex was added. The reaction mixture was incubated at room temperature for 1 h and loaded onto a native 12% acrylamide vertical gel (1/19 bisacrylamide) in Tris−borate−EDTA (TBE) buffer, supplemented with 20 mM KCl. The reaction was terminated by addition of 8 μL of gel loading buffer (30% glycerol, 0.1% bromophenol blue, 0.1% xylene cyanol), and the subsequent solution (10 μL) was analyzed on a 12% native PAGE (the gel was prerun for 30 min). Electrophoresis was performed at 4 °C in TBE buffer (pH 8.3) containing 20 mM KCl for 15 h. The gels were dried and visualized with a PhosphorImager.

Ligase Assay. For each ligation reaction, 10 μL of ^{32}P-labeled DNA (5 ng) was mixed with 10 μL of 100 mM KCl solution. The mixture was boiled for 10 min and cooled to 25.0 °C. A 2 μL portion of a 10× ligase buffer (500 mM Tris−HCl, 100 mM $MgCl_2$, 100 mM DTT, 10 mM ATP, 500 μg/mL BSA, pH 7.8) and 1 μL of ligase were added. The reaction was incubated at 16.0 °C overnight and inactivated by heating to 70.0 °C for 20 min. The samples were subjected to phenol extraction and ethanol precipitation and analyzed with 8% denaturing PAGE.

Absorption Titration. Solutions of the platinum(II) complexes (50 μM) were prepared in Tris/KCl buffer (100 mM KCl, 10 mM Tris HCl, pH 7.5), and aliquots of a millimolar stock G-quadruplex DNA solution (0−1000 μM) were added. Absorption spectra were recorded in the 200−600 nm range, after equilibration at 20.0 °C for 10 min. The intrinsic binding constant, K, was determined from a $D/\Delta\varepsilon_{ap}$ vs D plot according to[37]

$$D/\Delta_{\varepsilon ap} = D/\Delta\varepsilon + 1/[(\Delta\varepsilon)K] \quad (1)$$

where D is the concentration of DNA, $\Delta\varepsilon_{ap} = |\varepsilon_A - \varepsilon_F|$, $\varepsilon_A = A_{obs}/$[complex], $\Delta\varepsilon = |\varepsilon_B - \varepsilon_F|$, and ε_B and ε_F correspond to the extinction coefficients of the DNA−complex adduct and unbound complex, respectively.

UV Melting Study. Solutions of the G4A1-quadruplex in the absence and presence of the platinum complex [G4A1-quadruplex/metal complex = 1/1] were prepared in a buffer solution (10 mM Tris−HCl, pH 7.5, 100 mM KCl or NaCl). The temperature of the solution was increased at a 1 °C min^{-1} interval, and the absorbance at 295 nm was continuously monitored. The T_m values were determined graphically from the plots of absorbance vs temperature.

Emission Titration. Solutions of the platinum(II) complexes (50 μM) were prepared in Tris/KCl buffer (100 mM KCl, 10 mM Tris−HCl, pH 7.5). Aliquots of a millimolar stock G-quadruplex DNA solution (0−1000 μM) were added. Emission spectra were recorded in the 400−800 nm range, after equilibration at 20.0 °C for 10 min.

G-Quadruplex DNA Detection in PAGE. After electrophoresis, the gels were stained with **1** at room temperature. Complex **1** was first dissolved in DMSO/MeOH (1 mL/2 mL) followed by addition of H_2O (17 mL). The gels were incubated with these solutions for 30 min with gentle agitation. Detection and imaging of the gels were conducted using the Alpha DigiDoc FC imaging system with Alpha DigiDoc AD-1200 software. The intensities of the DNA bands were recorded using the autospot function.

Competition Dialysis Assay.[25] A portion (400 mL) of the buffer solution (6 mM Na_2HPO_4, 2 mM NaH_2PO_4, 1 mM Na_2EDTA, 185 mM NaCl, pH 7.0, or Tris/KCl) containing 1 μM platinum(II) complex was used for each competition dialysis experiment. A volume of 200 μL at 75 μM monomeric unit of each of the DNA samples was pipetted into a separate dialyzer unit (Pierce). All eight dialysis units were placed in the beaker containing the buffer solution. The solution mixture was allowed to equilibrate with continuous stirring at room temperature (20−22 °C) for 48 h. At the end of the equilibration period, DNA samples were carefully transferred to microfuge tubes and treated with 1% SDS. The total concentration of platinum complex (C_t) within each dialysis unit was determined by the absorbance at 382 nm using $\varepsilon_{max} = 3500$ dm^3 mol^{-1} cm^{-1}. The concentration of the free platinum complex (C_f) was determined spectrophotometrically using an aliquot of the buffer solution. The amount of bound platinum complex (C_b) was determined according to

$$C_t - C_f = C_b \quad (2)$$

Assay of Telomerase Activity.[28] Telomerase activity in human tumor cell lines was measured using the non-PCR-based telomerase assay with 5′-biotinylated d(TTAGGG)$_3$. Cells extracts were prepared from 1×10^7 cells. The cultured HeLa cells were washed once in PBS (400 μL) and centrifuged at 10000g for 1 min at 4 °C, resuspended in 1.5 mL tubes containing 400 μL of ice-cold washing buffer [10 mM HEPES−KOH (pH 7.5), 1.5 mM $MgCl_2$, 10 mM KCl, and 1 M DTT], and then centrifuged again at 10000g for 1 min at 4 °C. The washed cells were resuspended in 100−400 μL of ice-cold lysis buffer [10 mM Tris−HCl (pH 7.5), 1 mM $MgCl_2$, 1 mM EDTA, 0.1 mM phenylmethylsulfonyl fluoride, 5 mM β-mercaptoethanol, 1 mM DTT, 0.5% 3-[(3-cholamidopropyl)dimethylammonio]-1-propanesulfonate (CHAPS), 10% glycerol (10^6 cells/20 μL of buffer)]. The suspension was incubated on ice for 60 min, and the lysate was centrifuged at 100000g at 4 °C in an ultracentrifuge for 1 h. The supernatants were stored at −80 °C in 10% glycerol.

Briefly, the reaction mixtures (20 μL) containing 4 μL of cell lysate, 50 mM Tris acetate (pH 8.5), 50 mM potassium acetate, 1 mM $MgCl_2$, 5 mM β-mercaptoethanol (BME), 1 mM spermidine, 1 μM telomere primer, 2.4 μM [α-^{32}P]dGTP (800 Ci/mmol), 1 mM dATP, 1 mM dTTP, and the Pt^{II} complex (0−6 μM) were incubated at 37 °C for 1 h. The reactions were terminated by adding 20 μL of prewashed streptavidin-coated Dynabead suspension containing 10 mM Tris−HCl (pH 7.5) and 2 M NaCl. The complex was separated from the suspension using a magnet and washed at least five times with buffer (1 M NaCl, 10 mM Tris−HCl, pH 7.5) to eliminate [α-^{32}P]dGTP background and nonspecific high molecular weight DNA. Telomerase reaction products were resuspended in 200 μL of 5.0 M guanidine−HCl at 90 °C for 20 min. The bead-reaction products were dissociated from the Dynabeads by placing the tubes in a magnetic rack, and the supernatant was transferred to a new tube. After ethanol precipitation, the reaction products were analyzed by 8% PAGE. Telomerase activity in HeLa cells was used for reference and defined as 100% activity. The $^{tel}IC_{50}$ values were determined by plotting the data using Excel Fit software.

Cytotoxicity Test by MTT Assay [3-(4,5-Dimethylthiazol-2-yl)-2,5-tetrazolium Bromide].[38] Briefly, cells were seeded in a 96-well flat-bottomed microplate at 20 000 cells/well in 150 μL of growth medium solution [10% fetal calf serum (FCS; Gibco), 1% Sigma A-7292 antibiotic and antimycotic solution in minimal essential medium (MEM-Eagle; Sigma)]. Complexes **1**−**7** and cisplatin (positive control) were dissolved in DMSO and mixed with the

(37) Kumar, C. V.; Asuncion, E. H. *J. Am. Chem. Soc.* **1993**, *115*, 8547.

growth medium (final concentration ≤4% DMSO). Aliquots of 100 μL of medium containing graded concentrations of the investigational compound were added to the microplate. The microplate was incubated for 48 h at 37 °C, 5% CO_2, and 95% air in a humidified incubator. After incubation, 10 μL of MTT reagent (5 mg/mL) was added to each well. The microplate was then reincubated at 37 °C in 5% CO_2 for 4 h. A 100 μL sample of solubilization solution (10% SDS in 0.01 M HCl) was added to each well. The microplate was left in the incubator for 24 h. Absorbances at 550 nm were measured on a microplate reader. The IC_{50} value (concentration required to reduce the absorbance by 50% compared to the controls) of each complex was determined by the dose dependence of surviving cells after exposure to the metal complex for 48 h.

NMR Experiments. ^{1}H NMR experiments were performed with a Bruker DRX500 or AV600 spectrometer. Typical acquisition conditions for a ^{1}H NMR spectrum were 45° pulse length, 2.0 s relaxation delay, 16K data points, 16−32 transients, and G4A3-quadruplex/G4A4-quadruplex in 90% H_2O/10% D_2O with 150 mM KCl, 25 mM KH_2PO_4, and 1 mM EDTA (pH 7.0). Aliquots of stock solutions of **1** were titrated directly to the DNA solution inside an NMR tube. Spectra were recorded at 300 K utilizing a standard jump−return pulse sequence for water suppression with a relaxation delay of 2 s.

Molecular Modeling. A model study on the stacking interaction between **1** and G-quadruplex DNA was performed. This was done using Gaussian 03. The platinum complex was optimized using DFT with a LanL2MB basis set.[39] The optimized structure of the platinum complex was used to do the docking. Molecular docking was performed using the ICM-Pro 3.4-8a program (Molsoft).[40] According to the ICM method, the molecular system was described using internal coordinates as variables. Energy calculations were based on the ECEPP/3 force field with a distance-dependent dielectric constant. The biased probability Monte Carlo (BPMC) minimization procedure was used for global energy optimization. The BPMC global energy optimization method consists of the following steps: (1) a random conformation change of the free variables according to a predefined continuous probability distribution; (2) local energy minimization of analytical differentiable terms; (3) calculation of the complete energy including nondifferentiable terms such as entropy and solvation energy; (4) acceptance or rejection of the total energy based on the Metropolis criterion and return to step 1. The binding between **1** and DNA was evaluated by binding energy, including grid energy, continuum electrostatic, and entropy terms. The DNA crystal structures for $d(T_2AG_3T)_4$ (PDB code 1NP9)[41] and the G4A2-quadruplex (PDB code 1KF1)[42] and the NMR structure for the G4A4-quadruplex (PDB code 2A5P)[26] were downloaded from the Protein Data Bank. Hydrogen and missing heavy atoms were added to the receptor structure followed by local minimization using the conjugate gradient algorithm and analytical derivatives in the internal coordinates. In the docking analysis, the binding site was assigned across the entire structure of the DNA molecule. The ICM docking was performed to find the most favorable orientation. The resulting **1**−G-quadruplex DNA complex trajectories were energy minimized, and the interaction energies were computed.

[Pt(dppz-COOH)(N^C)]CF_3SO_3 (1). An acetonitrile solution (50 mL) of Bu_4N[Pt(N^C)Cl_2] (0.46 g, 0.70 mmol) and $AgCF_3SO_3$ (0.36 g, 1.40 mmol) was refluxed for 4 h. The AgCl formed was filtered through Celite, and dppz-COOH (0.23 g, 0.70 mmol) was added to the filtrate. The resulting mixture was refluxed for 12 h. The volume of the solution was reduced to 5 mL, and diethyl ether was added to give a yellow precipitate, which was filtered and washed with diethyl ether (2 × 5 mL). Recrystallization by diffusion of diethyl ether into a CH_3CN solution afforded a yellow crystalline solid. Yield: 0.39 g, 70%. FAB-MS: *m*/*z* 674 [M^+]. ^{1}H NMR (500 MHz, CD_3CN): δ 7.05−7.40 (m, 2H), 7.50 (m, 2H), 7.55−7.77 (m, 2H), 7.90 (m, 2H), 8.00−8.20 (m, 2H), 8.20−8.30 (m, 2H), 8.55−8.65 (m, 2H), 9.08 (m, 1H), 9.75 (m, 2H). Anal. Calcd for $C_{31}H_{18}N_5SF_3O_5Pt$: C, 45.15; H, 2.20; N, 8.49. Found: C, 45.43; H, 2.55; N, 8.74.

[Pt(dppx)(N^C)]CF_3SO_3 (2). The procedure is similar to that of **1**, except that dppx (0.22 g, 0.70 mmol) was used. Yield: 0.47 g, 83%. FAB-MS: *m*/*z* 659 [M^+]. ^{1}H NMR (500 MHz, DMSO-d_6): δ 2.63 (s, 6H), 7.05−7.40 (m, 4H), 7.50 (m, 2H), 7.55−7.75 (m, 2H), 7.80 (m, 2H), 8.00−8.25 (m, 2H), 9.05−9.27 (m, 2H), 9.67 (m, 2H). Anal. Calcd for $C_{32}H_{22}N_5SF_3O_3Pt$: C, 47.53; H, 2.74; N, 8.66. Found: C, 47.06; H, 2.44; N, 8.97.

[Pt(dppc)(N^C)]CF_3SO_3 (3). The procedure is similar to that of **1**, except that dppc (0.25 g, 0.70 mmol) was used. Yield: 0.45 g, 76%. FAB-MS: *m*/*z* 700 [M^+]. ^{1}H NMR (500 MHz, DMSO-d_6): δ 7.05−7.30 (m, 4H), 7.40 (m, 2H), 7.75−7.80 (m, 2H), 8.00−8.25 (m, 2H), 8.50−8.75 (m, 2H), 9.05−9.27 (m, 2H), 9.50 (m, 2H). Anal. Calcd for $C_{30}H_{16}N_5Cl_2SF_3O_3Pt$: C, 42.41; H, 1.89; N, 8.24. Found: C, 42.36; H, 1.70; N, 8.05.

[Pt(dppz)(Thpy)]CF_3SO_3 (4). A CH_3CN solution (50 mL) of Bu_4N[Pt(Thpy)Cl_2] (0.46 g, 0.70 mmol) and $AgCF_3SO_3$ (0.36 g, 1.40 mmol) was refluxed for 4 h. The AgCl formed was filtered through Celite, and dppz (0.2 g, 0.70 mmol) was added to the filtrate. The resulting mixture was refluxed for 12 h. The volume of the solution was reduced to 5 mL, and diethyl ether was added to give a yellow precipitate, which was filtered and washed with diethyl ether (2 × 5 mL). Recrystallization by diffusion of diethyl ether into a CH_3CN solution afforded an orange crystalline solid. Yield: 0.44 g, 80%. FAB-MS: *m*/*z* 637 [M^+]. ^{1}H NMR (500 MHz, DMSO-d_6): δ 6.92 (d, 1H, *J* = 7.7 Hz), 6.99 (d, 2H, *J* = 5.3 Hz), 7.44 (d, 1H, *J* = 4.6 Hz), 7.68−7.73 (m, 1H), 7.88−7.93 (m, 1H), 7.96−8.04 (m, 3H), 8.11−8.22 (m, 2H), 8.30 (d, 1H, *J* = 5.3 Hz), 9.00 (d, 1H, *J* = 4.6 Hz), 9.33 (d, 2H, *J* = 7.5 Hz), 9.43 (d, 1H, *J* = 7.9 Hz). Anal. Calcd for $C_{28}H_{16}N_5S_2F_3O_3Pt$: C, 42.75; H, 2.05; N, 8.90. Found: C, 42.55; H, 2.20; N, 9.03.

[Pt(dppp2)(N^C)]CF_3SO_3 (5). The procedure is similar to that of **1**, except that dppp2 (0.20 g, 0.70 mmol) was used. Yield: 0.47 g, 86%. FAB-MS: *m*/*z* 632 [M^+]. ^{1}H NMR (500 MHz, DMSO-d_6): δ 7.05−7.40 (m, 4H), 7.50 (m, 2H), 7.52−7.75 (m, 2H), 7.80 (m, 1H), 8.00−8.25 (m, 2H), 8.50−8.75 (m, 2H), 9.05−9.28 (m, 2H), 9.50−9.80 (m, 2H). Anal. Calcd for $C_{29}H_{17}N_6SF_3O_3Pt$: C, 44.56; H, 2.19; N, 10.75. Found: C, 44.77; H, 2.31; N, 10.61.

Acknowledgment. This work was supported by the Area of Excellence Scheme established under the University Grants Committee of the Hong Kong Special Administrative Region, China (Grant AoE/P-10/01), and The University of Hong Kong (University Development Fund).

Supporting Information Available: Figures S1−S20, Tables S1−S5, and Scheme S1. This material is available free of charge via the Internet at http://pubs.acs.org.

JA806045X

(38) Mosmann, T. *J. Immunol. Methods* **1983**, *65*, 55.
(39) (a) Hay, P. J.; Wadt, W. R. *J. Chem. Phys.* **1985**, *82*, 270. (b) Wadt, W. R.; Hay, P. J. *J. Chem. Phys.* **1985**, *82*, 284. (c) Hay, P. J.; Wadt, W. R. *J. Chem. Phys.* **1985**, *82*, 299.
(40) Totrov, M.; Abagyan, R. *Proteins, Suppl.* **1997**, *1*, 215.
(41) Gavathiotis, E.; Searle, M. S. *Org. Biomol. Chem.* **2003**, *1*, 1650.
(42) Parkinson, G. N.; Lee, M. P.; Neidle, S. *Nature* **2002**, *417*, 876.